UDK 621.74.043:669.018.258
Original scientific article/Izvirni znanstveni članek

ISSN 1580-2949
MTAEC9, 48(5)735(2014)

INFLUENCE OF THE WORKING TECHNOLOGY ON THE DEVELOPMENT OF ALLOYS H13-*w*(Cu) 87.5 %

VPLIV TEHNOLOGIJE IZDELAVE NA RAZVOJ ZLITINE H13-*w*(Cu) 87,5 %

Uroš Artiček[1], Marko Bojinovič[2], Mihael Brunčko[3], Ivan Anžel[3]

[1]EMO – Orodjarna, d. o. o., Bežigrajska cesta 10, 3000 Celje, Slovenia
[2]TIC-LENS, d. o. o., Bežigrajska cesta 10, 3000 Celje, Slovenia
[3]Faculty of Mechanical Engineering, University of Maribor, Smetanova 17, 2000 Maribor, Slovenia
uros.articek@gmail.com

Prejem rokopisa – received: 2013-11-04; sprejem za objavo – accepted for publication: 2013-11-22

Most dies in the casting industry for injection moulding are machined from the premium-grade H13 tool steel. They provide excellent performance in terms of mechanical properties and service life; however, these dies are characterised by a relatively low thermal conductivity. The tool-and-die industry is interested in depositing a material of a high thermal conductivity onto steel in order to improve the thermal management and productivity. We have explored the possibility of using copper with a new technology. In this study, the microstructure evolution and mechanical properties are discussed using the Laser Engineered Net Shaping™ (LENS™) technology. For a better understanding of the solidification, the microstructure of a LENS sample was compared with the microstructure of a reference alloy produced with the ingot-casting technology having the same chemical composition of H13-*w*(Cu) 87.5 %. We carried out light microscopy, scanning electron microscopy, an EDS microchemical analysis, the tensile test and microhardness testing. The results show a successful fabrication of LENS samples; their microstructure is more homogeneous compared to the castings; they show better mechanical properties and represent a good potential for further development and use.

Keywords: LENS, casting, microstructure evolution, mechanical properties

V industriji tlačnega litja se za izdelavo matric orodij pogosto uporablja visokokakovostno orodno jeklo H13, ki ima odlične mehanske lastnosti in dolgo trajnostno dobo, vendar je zanj značilna relativno nizka toplotna prevodnost. Orodjarska industrija želi dodati jeklu material z visoko toplotno prevodnostjo za dosego boljše porazdelitve toplote in večje produktivnosti. Z novo tehnologijo, imenovano Laser Engineered Net Shaping™ (LENS™), smo raziskali možnost uporabe bakra, spremljali razvoj mikrostrukture ter ugotovili mehanske lastnosti. Za boljše razumevanje strjevanja smo primerjali mikrostrukturo vzorca LENS z mikrostrukturo referenčne zlitine z enako kemijsko sestavo H13-*w*(Cu) 87,5 %, izdelano s tehnologijo litja. Karakterizacija zlitin je potekala s svetlobno mikroskopijo, vrstično elektronsko mikroskopijo, mikrokemično EDS-analizo, z nateznim preizkusom in merjenjem mikrotrdote. Rezultati kažejo uspešno izdelavo vzorcev LENS, katerih mikrostruktura je bolj homogena in ima boljše mehanske lastnosti v primerjavi z odlitki. Tehnologija LENS je dober potencial za nadaljnji razvoj in uporabo v praksi.

Ključne besede: LENS, litje, razvoj mikrostrukture, mehanske lastnosti

1 INTRODUCTION

In the injection-moulding industry, new materials and technologies are required for mould dies in order to optimize the production and keep the costs as low as possible. Despite their excellent mechanical properties, tool steels that are nowadays used as the materials for moulds limit the productivity due to their low thermal conductivity. To solve this problem, designers have been focusing on how to design the tool geometry and construction to achieve higher cooling rates. Complex cooling channels are being designed to enable the cooling liquid to extract the heat from a mould. Ejector pins, slides and air-stream gates are used to eject a part from a mould cavity so the space left in it is small. An alternative way to solve this problem is the use of copper-beryllium inserts[1], which have a higher thermal conductivity. However, they can leave marks on the part and are not environmentally friendly.

Therefore, new technologies and materials, like a Cu-deposition on tool steel, or functionally graded materials (FGM) with a combination of high strength, wear resistance and thermal conductivity are explored as potential candidates for a more efficient injection-moulding tool. The use of a direct-metal-deposition (DMD) fabrication process makes it possible to create an optimum configuration of fin trees and cooling channels as well as to use FGM without being concerned with the limitations of the traditional manufacturing method[2,3]. The laser-engineered-net-shaping™ (LENS) process is seen as one of the most promising DMD technologies for the production of such materials[4–6]. LENS is a relatively new technology capable of rapidly producing complex, fully dense parts directly from a computer-aided design (CAD). A high-power Nd-YAG laser is used to heat and melt a metal powder, thereby producing a melt pool on a substrate attached to an X-Y table. The metal powder from coaxial powder-feed nozzles is injected into the melt pool as the table is moved along pre-designed 2-D tool paths generated using the sliced CAD models. The additions of multiple layers produce a 3-D net or a near-net shape. The fabrication takes place under a controlled,

Table 1: Chemical composition of tool steel H13 in mass fractions, *w*/%
Tabela 1: Kemijska sestava orodnega jekla H13 v masnih deležih, *w*/%

Element	C	Si	Mn	Cr	Ni	Mo	V	Fe
Composition (*w*/%)	0.32 - 0.45	0.8 - 1.2	0.2 - 0.5	4.75 - 5.5	0.3 max	1.1 - 1.75	0.8 - 1.2	bal.

inert atmosphere of argon. Some of the important process parameters are laser power, powder flow rate, layer thickness, hatch width, deposition speed and oxygen level.

The iron-copper (Fe-Cu) alloying system[7] is one of the most suitable systems to produce an efficient FGM mould material. The thermal conductivity of copper is approximately 13 times higher than that of the H13 tool steel at the operating temperatures between 220–600 °C. Unfortunately, a large solidification temperature range and a high amount of the Cu-rich terminal liquid over a wide range of Cu concentration promote solidification cracking in Fe-Cu alloys[8,9]. Additionally, a Fe-Cu phase diagram contains two peritectics and a nearly flat liquidus; they exhibit a high tendency for non-equilibrium solidification that probably has a significant influence on the susceptibility to cracking[7,8]. At the same time, LENS is considered to be a technology that involves a high velocity of solidification with the possibilities of specific reactions, new phases and a metastable microstructure formation. While the properties of materials mainly depend on the microstructures, it is important to know the microstructure development during the LENS process as well as the final microstructure of the layers, depending on the thermal influence of the additional layers.

Our main objective is to explore the microstructure development with the LENS technology. As it is evident from the previous research[8], some chemical compositions are more susceptible to the formation of cracks when using DMD in a Fe-Cu system. Based on the current data, it is not yet possible to conclude how the LENS technology will influence the formation of cracks. In the first part of our research, the composition of H13-*w*(Cu) 87.5 % was selected. Despite the fact that this composition belongs to the crack-free composition range, the question of how the LENS technology influences the microstructure evolution is still open. Namely, the thermal impact of the solidifying layers on the microstructure of the previously solidified layers and the irregularities of the previous layers is not yet known. In our research, the resulting microstructures and mechanical properties of the samples produced in this way were compared with the conventional-casting samples with the same composition, which enabled us to evaluate the effect and the rationality of the technology.

2 EXPERIMENTAL WORK

The conventional solidification of the alloying system consisting of the H13 tool steel and the mass fraction of Cu w = 87.5 % was studied using the mould casting. For the preparation of the alloy, oxygen-free high-conductivity copper (w (Cu) = 99.99 %) and the H13 tool steel with the chemical composition presented in **Table 1** were used. The material system was vacuum-induction heated at 10^{-2} mbar. Before melting, the chamber was backfilled with the high-purity Ar gas up to 1150 mbar. The melt was homogenized at 1450 °C and then cast at 1400 °C into, cylindrically shaped, grey-cast-iron moulds 50 mm. The inner walls of the moulds were protected with a thin layer of ZrO_2. Before casting, the moulds were preheated to 400 °C to decrease the cooling rate and lower the melt undercooling prior to the primary solid nucleation.

For the layered manufacturing experiments a LENS 850-R machine made by Optomec Inc. with a high-power Nd:YAG laser with a capacity of 1000 W was used. The machine consists of a dual-powder feeder system that allows a simultaneous delivery of two different material mixtures. Several cylindrically shaped samples (D = 10 mm, L = 100 mm) were successfully produced using the following parameters: the laser power of 530 W, the traverse speed of 5.3 mm/s, the layer thickness of 0.35 mm, the hatch spacing of 0.46 mm, the hatch angle of 60° and the powder-flow rate of 2.75 g/min. In our experiments, we used the powders produced using gas atomisation with the particle sizes ranging from 45 μm to 160 μm (**Figure 1**). The greater

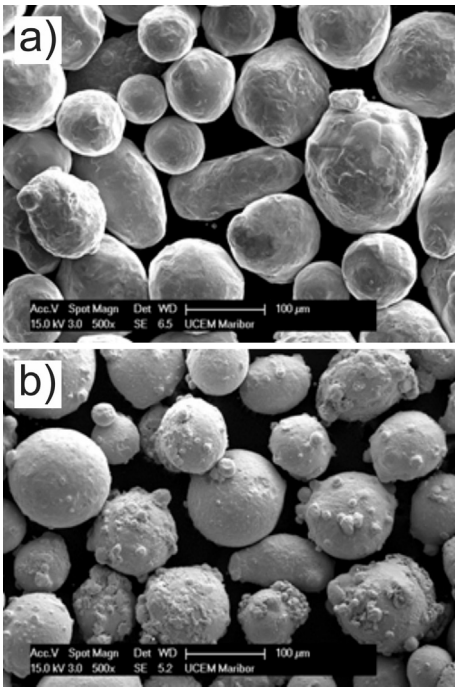

Figure 1: SEM images of the powders: a) Cu, b) tool steel H13
Slika 1: SEM-posnetka prahov: a) Cu, b) orodno jeklo H13

parts of the powders of both materials were spherical, providing the solution to the porosity problem[10,11]. The powders were delivered by the argon carrier gas (2 L/min) to the focus of the laser beam. The oxygen level during all the experiments was maintained below $10 \cdot 10^{-6}$.

The influence of the microstructure on the mechanical properties was evaluated using uniaxial tensile testing and microhardness measurements. The static tensile tests were performed on a Zwick/Roell ZO 10 tensile-testing machine with a load cell capacity of 10 kN at a constant position and a controlled speed of the crosshead of v = 1.5 mm/min at ambient temperature. The shapes and dimensions of the tensile-test samples complied with the SIST EN 10002-1 standard. The mechanical properties of several testing samples cut out from the cylinder-shaped casting produced with the conventional casting technology were compared with the tensile bars obtained with the LENS technology, machined in the longitudinal orientation so that the axis of the tensile bars was parallel to the cladding direction. The hardness measurements were carried out according to the 6507-1:1998 standard by means of the Vickers test on a Zwick 3212 microhardness-measurement device.

A microstructural characterisation of the conventionally cast and LENS materials was carried out with light microscopy, LM (Nikon Epiphot 300) and scanning electron microscopy, SEM (FEG Sirion 400 NC) as well as the energy dispersive X-ray analysis, EDX (INCA 6650). The samples for light and electron microscopies were grinded, polished and etched according to the standard metallographic procedures. The etching in a solution consisting of 5 g $FeCl_3$, 10 mL HCl and 100 mL ethanol for about 20 s was used to reveal the microstructure.

3 RESULTS AND DISCUSSION

The microstructure evolution during solidification depends on the alloy characteristics, its chemical composition and it is primarily a function of the solidification condition. For a better understanding of the solidification process under the LENS conditions, the microstructure obtained with conventional solidification in the mould casting of an alloying system with the same composition was studied first.

3.1 Microstructure of conventional-casting samples

The typical microstructure of the conventionally cast material composed of the H13 tool steel and w(Cu) = 87.5 % is shown in **Figure 2**. The microstructure consists of the Fe-rich dendritic-like primary phase (P1) and Cu-rich matrix (M1). However, the size, morphology and distribution of the primary-phase particles are very different throughout the volume of the casting, indicating a high inhomogeneity of the microstructure.

A detailed microstructural analysis of the samples at a higher magnification revealed very fine dendrites (P2) in the Cu-rich matrix and the Cu-rich zone (M2) around the Fe-rich particles (**Figure 3**). An elemental EDX analysis performed within the FE SEM indicates that the Fe-rich primary phase and the surrounding zone contain the alloying elements of the H13 tool steel, while the Cu-rich matrix and fine dendrites consist only of copper and iron (**Table 2**). Because of the inaccuracy of the EDX method used for a quantitative analysis of light

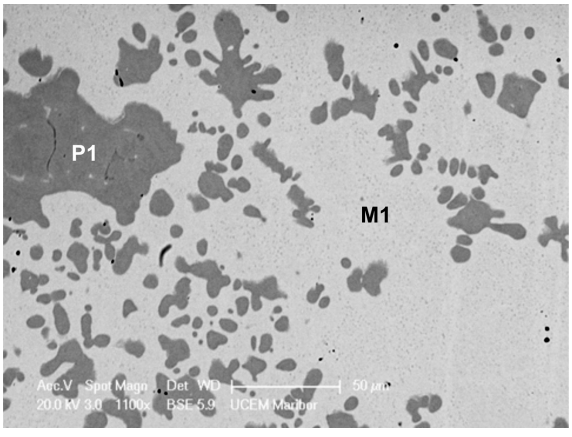

Figure 2: Microstructure of the as-cast sample (SEM back-scattered electron image – BEI)

Slika 2: Mikrostruktura litega vzorca (SEM-posnetek povratno sipanih elektronov – BEI)

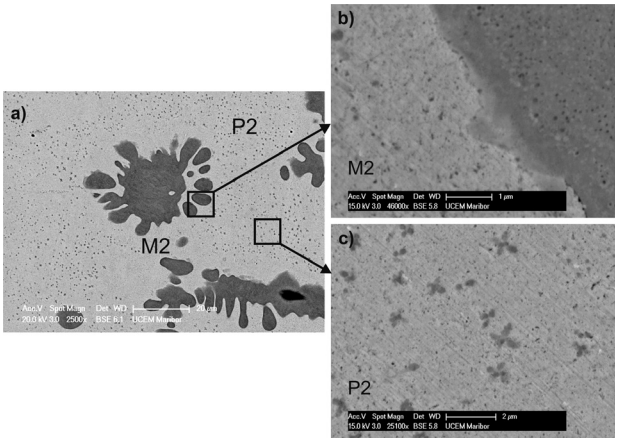

Figure 3: SEM BEI of the: a) as-cast sample, b) showing the Cu-rich zone around the Fe-rich particle and c) fine dendrites in the Cu-rich matrix

Slika 3: SEM BEI: a) litega vzorca, b) področje, bogato z bakrom, okrog delca, bogatega z železom, in c) fini dendriti v matrici, bogati z bakrom (c)

Table 2: Chemical compositions of different microstructural regions in mass fractions, *w*/%

Tabela 2: Kemijska sestava različnih področij mikrostrukture v masnih deležih, *w*/%

Microstructural region	Chemical composition (*w*/%)						
	Fe	Cu	Cr	Mo	Si	V	Mn
P1	78.9	14.5	3.8	1.2	0.6	0.9	0.1
M1	3.6	96.4					
M2	4.5	95.0	0.3		0.1		0.1

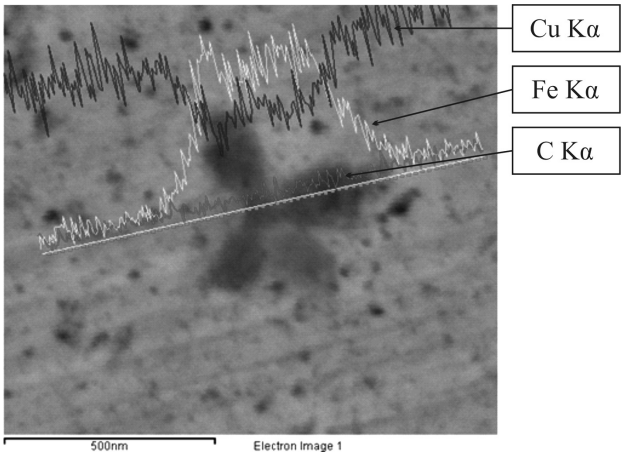

Figure 4: Line microanalysis across a fine dendrite in the Cu-rich matrix
Slika 4: Linijska mikroanaliza preko finega dendrita v matrici, bogati z bakrom

elements, the detected carbon concentration was not taken into consideration in these results. Also, in the microchemical analysis of fine dendrites, the size of the interaction volume was too large for a correct quantitative evaluation of the elements. Therefore, a line analysis is presented in **Figure 4** to show the detected chemical elements in the region of fine dendrites.

It is well known that the alloys from the ternary Cu-Fe-Cr system[12,13] indicate a high tendency for non-equilibrium solidification with metastable transformations. The phase diagrams of the constituent binary Cu-Fe and Cu-Cr systems have flat parts of the liquidus lines, and a metastable liquid-phase separation has been established for these systems[13,14]. The Cu-Fe system displays a large solidification-temperature range and a peritectic reaction at both ends of the phase diagram. Under the near-equilibrium condition, the solidification of the hypo-peritectic composition with w(Cu) = 87.5 % starts with the γ-Fe dendrite nucleation. A further cooling leads to the growth of the primary phase, and the solidification ends with a peritectic reaction, where the rest of the remaining liquid reacts with an equivalent part of the primary solid, i. e., γ-Fe + L → ε-Cu. On the other hand, if the melt is undercooled below the metastable miscibility gap, the metastable liquid-phase separation takes place, i. e., L → L1 (Fe-rich) + L2 (Cu-rich). In this case, the L1 phase solidifies as the leading phase under the non-equilibrium conditions and the solidification of the L2 phase proceeds under the near-equilibrium condition.

According to the Cu-Fe binary-phase diagram with metastable miscibility lines, the minimum undercooling which is required for the liquid-phase separation depends on the chemical composition[15]. For the alloy with w(Cu) = 87.5 %, the estimated critical value of ΔT based on the metastable miscibility line in the phase diagram is about 70 K. An addition of Cr increases the critical temperature of the miscibility gap of the Cu-Fe binary system[15,16] and decreases the necessary undercooling for the metastable liquid separation.

The results of our microstructural analysis indicate that the obtained undercooling in the mould casting of the material composed of the H13 tool steel and w(Cu) = 87.5 % exceeded the critical value for the melt separation into two liquids: Fe-rich and Cu-rich. After the separation, both liquid phases were undercooled. In accordance with different copper concentrations, the Fe-rich liquid was more undercooled, having a larger driving force for nucleation. Consequently, the solidification started with the Fe-rich primary-phase nucleation in the Fe-rich liquid. The lower undercooling as well as the recalescence event during the Fe-rich liquid solidification enabled the Cu-rich liquid to solidify at a much smaller deviation from equilibrium. The composition and fraction of each liquid changed as the sample was being continuously cooled and probably followed the metastable miscibility-gap phase boundary as the time was allowed for the transfer of the atoms between the two liquids. The solidification of both liquids was terminated by a peritectic reaction, which resulted in the formation of a Cu-rich zone around the Fe-rich primary phase.

3.2 Microstructure of LENS samples

The LENS process can be analysed as a sequence of discrete events, given that it is a layer-by-layer process. Each layer of the melted powders composed of H13-w(Cu) 87.5 % was highly supercooled below the liquidus temperature; the liquid entered an immiscibility gap and separated into two liquids[17]. The phase separation generally appeared as dispersed Fe-rich liquid spheres (L1) in the Cu-rich liquid matrix (L2). **Figure 5** shows a typical microstructure of a LENS sample in the longitudinal direction. The microstructure is not fully homogeneous, but still much more homogeneous than in the cast samples. It consists of dark and bright areas

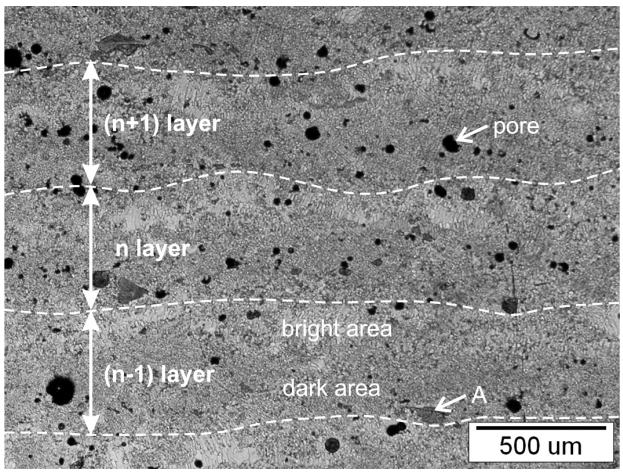

Figure 5: Typical microstructure of a LENS sample layer deposition in the longitudinal direction
Slika 5: Tipična mikrostruktura vzdolžnega prereza vzorca plastne gradnje procesa LENS

depending on the distribution and size of the Fe-rich phase, which are a consequence of the heat-affected zone (HAZ) and re-melting zone (RMZ). The dark (wide) area consists of fine copper grains, dispersed fine spherical particles of the Fe-rich phase and some individual coarse Fe-rich particles. In the bright (tight) area – the interlayer zone – the copper grain sizes are bigger, and the area includes a considerably lower amount of Fe-rich spherical particles that are also of a smaller size. There are no individual coarse Fe-rich particles.

If we compare the average size of the dendritic-like primary phase in the as-cast microstructure, being in the range of 100 μm, with small Fe-rich spherical-type particles of the LENS samples, we can see that they are much smaller (2–8 μm) and also more uniformly distributed. The size of these Fe-rich particles depends on the dark/bright area of the microstructure. Some individual coarse Fe-rich particles (A) can also be observed, but they occur less often, normally in the dark area of the microstructure, and belong to the size range of 100 μm (**Figure 5**).

In the microstructure, a uniformly distributed micro-spherical-type gas porosity is present. The gas dissolved or entrapped in the melt did not have sufficient time to escape to the top of the melt pool due to a rapid solidification. However, the concentration of porosity is much smaller than it can often be because of the spherical morphology of atomized powders[10,11]. An light micrograph (**Figure 5**) clearly shows the presence of porosity, indicated by small dark spots, having a diameter smaller than 50 μm.

For a better understanding of the microstructure evolution, we clad one single layer on the substrate. In this case, the primary microstructure was preserved because there was no HAZ or RMZ caused by additional layers. The temperature distribution was different. The absence of HAZ and RMZ, and significantly higher cooling rates because of the cold-plate substrate prevented the Fe-rich liquid spheres (L1) from coarsening. There were no individual coarse Fe-rich particles. The results show that the resultant microstructure with a very fine grain size of approximately 1 μm is homogeneous, and the minority Fe-rich phase spheres are homogenously dispersed in the Cu-rich matrix so that there are no dark or bright areas (**Figure 6**).

A further deposition of layers led to the changes in the primary single-layer microstructure. As the previous layer was re-melted, some of the Fe-rich particles lifted up into the new layer due to the lower density of iron compared to copper. RMZ provides a directional solidification and a grain growth of Cu-crystals in the bright area. Ahead of the solid-liquid interface, liquid L1 becomes highly undercooled and begins to solidify forming a solid and dark area. The latent heat is released to the previous layer slowing down the growth of Cu in RMZ (**Figure 7a**). The figure shows the distribution and size of the Fe-rich particles in the Cu-rich matrix in the dark and bright areas of an individual clad layer, in which the bright area is in the upper part and the dark area in the lower part of **Figure 7b**.

The theoretical layer thickness is 355 μm. For the cyclical layer deposition technique, an interlayer zone – the bright area between two deposition layers – is characteristic, being a consequence of re-melting. The bright and dark areas depend on the local heat input and

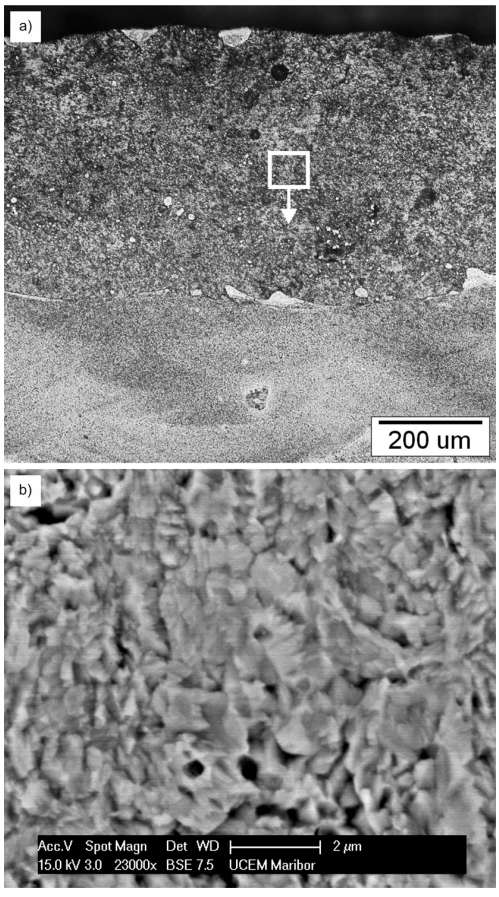

Figure 6: Single-layer weld build-up shows a very fine-grained microstructure: a) LM micrograph, b) SEM BEI micrograph

Slika 6: Ena sama navarjena plast izkazuje zelo finozrnato mikrostrukturo: a) LM-posnetek, b) SEM BEI-posnetek

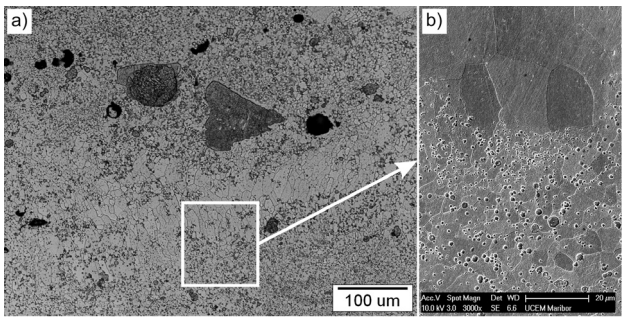

Figure 7: Border area of an individual layer recorded with: a) LM, and b) SEM micrograph of the transitional zone between a dark and a bright area

Slika 7: Mejno področje posamezne plasti, posneto z: a) LM in b) SEM-posnetek prehoda iz temnega v svetlo področje

the mechanism of the turbulence in the melt due to cladding the next layer (**Figure 5**).

After the liquid-phase separation, Fe-rich droplets grow and coagulate in order to reduce the interface area with the Cu-rich phase. Since the system still remained a complete liquid during the period between the separation and solidification, the liquid Fe-rich spheres can grow and move relative to the Cu-rich matrix and to each other.

Several mechanisms have been proposed to explain the evolution of size distribution of the dispersion phase, including the wetting behaviour, Ostwald ripening and coarsening of droplets due to collisions, whereby the size of the dispersed L1 spheres increases with the increasing undercooling. Generally, as the cooling rates become higher, the solidification time becomes shorter and the microstructure becomes finer[18]. The area with a higher amount of dispersed Fe-rich particles exhibits very fine grains of the Cu-rich matrix (**Figure 7**).

High undercooling favours a long interval between the separation and nucleation temperatures. As shown in the upper part of **Figure 8**, there was enough time for the spheres to grow through coagulation or coalescence. With the coalescence, some droplets collided with each other so that they may have mutually lost surface energy by joining to form a larger single one. Coagulation, on the other hand (a lower temperature, a higher viscosity) is a process when particles come together irreversibly, i.e., they get stuck together and cannot be separated. Coagulation and coalescence constitute a process, in which fine, dispersed, primary spherical Fe-rich particles (2–8 μm) aggregate together to form individual coarse Fe-rich particles that belong to the size range of 100 μm.

Furthermore, low undercooling provides a short coarsening time, in which a free movement and coagulation cannot occur. Therefore, the coarsening of the L1

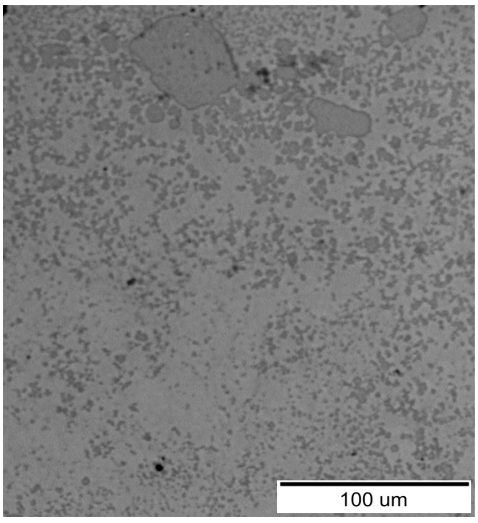

Figure 8: Coagulation and coalescence mechanisms in liquid-liquid mixtures and the Ostwald ripening mechanism in solid-liquid mixtures
Slika 8: Mehanizem koagulacije in koalescence v zmesi tekoče-tekoče in mehanizem Ostwaldovega zorenja v zmesi trdo-tekoče

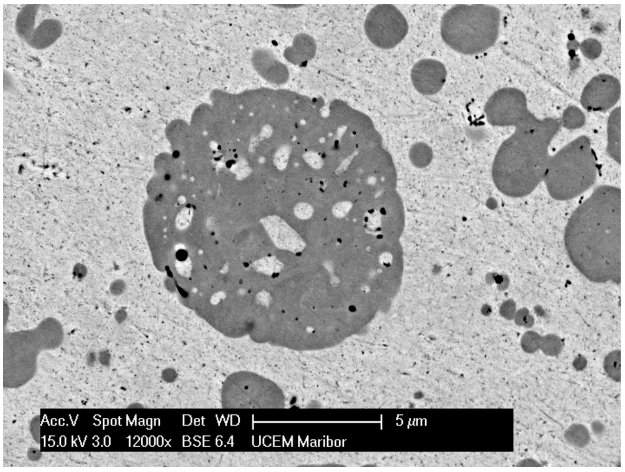

Figure 9: SEM BEI micrograph of a secondary phase separation inside an Fe-rich particle
Slika 9: SEM BEI-posnetek prikazuje sekundarno ločitev faze v delcu, bogatem z železom

spheres in this undercooling range should be attributed to Ostwald ripening[19]. This is a mechanism, allowing the droplets to coalesce due to the solute diffusion between them. The solute solubility depends on the curvature of a droplet; the smaller the curvature, the larger is the radius and the lower is the solubility. This diffusion-dependent coarsening mechanism plays a dominant role when the dispersion phase has a small diameter. With an increase in the droplet radius and a decrease in the temperature, the solid-liquid interface tension increases, whereas the solubility decreases, resulting in the weakening of Ostwald ripening. This mechanism can be observed in the lower part of **Figure 8**, in the bright area.

It should also be noted that the secondary phase separation was observed in the highly undercooled areas of the H13-*w*(Cu) 87.5 % alloy, i.e., inside the L1 phase, and some Cu-rich spheres occurred due to the secondary phase separation (**Figure 9**), which is a monotonic increasing function of undercooling. Multi-phase separation has been rarely observed in stable metallic immiscibles. Since liquid metals exhibit a low viscosity and high diffusion coefficient, less time is needed to adjust the composition of the primary phases[20]. However, as undercooling increases, the viscosity rises and diffusion coefficient declines. In this case, a complete diffusion is absent and a multi-phase separation in the liquid becomes more likely to occur.

3.3 Mechanical properties

The solidification parameters of the alloys directly affect the microstructures of the alloy systems, and also significantly influence their mechanical behaviours. The LENS samples have higher tensile-strength values and the cast samples are more ductile (**Figure 10**). This is due to their microstructures, which are finer and more homogenous in the LENS samples that solidified at much higher rates. The uniformly distributed particles of

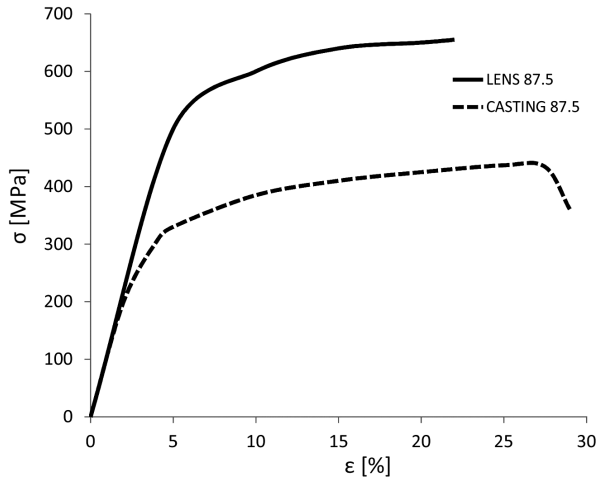

Figure 10: Stress-strain curves of the cast and LENS alloys at room temperature
Slika 10: Krivulja napetost – raztezek lite in LENS-zlitine pri sobni temperaturi

Table 3: Results of the average microhardness-measurement values according to Vickers
Tabela 3: Rezultati povprečnih vrednosti merjenja mikrotrdote po Vickersu

CASTING	of dendrites	near the dendrites	without dendrites
	194 HV 0.01	67 HV 0.01	49 HV 0.01
LENS	α_{Fe}	α_{Cu}	α_{Cu} (HAZ)
	734 HV 0.01	102 HV 0.01	81 HV 0.01

the Fe-rich phase, which are of a smaller size and in a larger quantity, represent the regions that require an increased amount of energy for the dislocations to pass through.

The elongation (ε) of cast samples is greater than the elongation of LENS samples. This is due to different solidification rates of the alloys. A LENS microstructure is the result of faster cooling and solidification – a metastable solidification where the Cu-rich matrix with a higher strength is formed (containing more alloying elements and precipitates due to which ε is smaller). In the case of cast samples where the solidification is slower, the matrix – practically pure copper – has a lower strength, resulting in a larger ε.

There is a trend of the LENS samples to have a slightly higher value of elastic modulus E than the cast samples because they are more metastable due to a greater number of the alloying elements in the Cu-rich matrix, affecting the bond strength.

These characteristics of the microstructure are reflected on the results of the microhardness measurements. A very fine-grained microstructure, a smaller size, a larger quantity of the uniformly distributed Fe-rich spherical phase and the amounts of the alloying elements in the Cu-rich matrix result in significantly higher average microhardness values of the LENS samples. **Table 3** shows the average measures of the microhardness values of the cast samples in the areas of dendrites, near dendrites and without dendrites and the microhardness of the LENS samples in Fe-rich phases, Cu-rich phases and the re-melted HAZ.

4 CONCLUSIONS

In this research, two different technologies were compared, i.e., the LENS technology and the conventional mould casting to produce an alloy with the same chemical composition, H13- *w*(Cu) 87.5 %. The obtained results can be summarized as follows:

- During the solidification of the conventional castings, the melt is undercooled and separated into two phases. The Fe-rich phase solidifies as the leading phase under the non-equilibrium condition and the solidification of the Cu-rich phase proceeds under the near-equilibrium condition according to the phase diagram.
- Large local variations in the temperature gradient of the castings cause a very inhomogeneous microstructure.
- The microstructure of the LENS samples is much more homogeneous than that of the cast samples. During the LENS process, where a much higher undercooling takes place, the undesired dendritic morphology of primary Fe-rich crystals becomes spherical.
- There is a significant change in the microstructure of a LENS sample between the first layer and the following layers that are re-melted and heat affected, resulting in dark and bright areas of the microstructure. The largest differences are due to HAZ, where a bright area occurs, containing a very small amount of Fe-rich spherical particles. The bright area represents the weaker part of the material, which should be minimized as much as possible by optimizing the energy intake. However, the microstructure is sufficiently homogeneous to allow homogeneous mechanical properties of the bulk samples.
- The porosity found in the LENS samples was considered low and uniformly distributed due to the spherical morphology of the atomized powders.
- The tensile data show that the as-deposited yield strength of the LENS fabricated materials is substantially higher than that of the cast materials; better properties are obtained as a result of a rapid solidification and grain refinement. The tensile data and microstructure characterisation indicate a good metallurgical bonding of individual layers of LENS deposits.
- It has been shown that the H13-*w*(Cu) 87.5 % alloy fabricated with the LENS technology can perform well in real-life applications. A good thermal conductivity of copper and a high wear resistance of steel can be achieved without any cracks as well as better

mechanical properties compared to conventional mould casting.

Acknowledgments

The research is partially funded by the European Social Fund. Invitations to tenders for the selection of the operations are carried out under the Operational Programme for Human Resources Development for 2007–2013, 1. development priority: Promoting entrepreneurship and adaptability, the priority guidelines, 1.1: Experts and researchers for enterprises to remain competitive.

5 REFERENCES

[1] J. C. Rebelo, A. M. Dias, R. Mesquita, P. Vassalo, M. Santos, An experimental study on electro-discharge machining and polishing of high strength copper–beryllium alloys, Journal of Materials Processing Technology, 103 (**2000**) 3, 389–397

[2] V. E. Beal, P. Erasenthiran, N. Hopkinson, P. Dickens, C. H. Aharens, Fabrication of x-graded H13 and Cu powder mix using high power pulsed Nd:YAG laser, Proc. of SolidFreeform Fabrication Symposium, Austin, Texas, 2004, 187–197

[3] W. Jiang, R. Nair, P. Molian, Functionally graded mold inserts by laser-based flexible fabrication: processing modeling, structural analysis, and performance evaluation, Journal of Materials Processing Technology, 166 (**2005**) 2, 286–293

[4] Optomec, Additive manufacturing system, Laser Engineered Net ShapingTM [online], 2006 [25. 8. 2013], available from the World Wide Web: http://www.optomec.com/Additive-Manufacturing-Technology/Laser-Additive-Manufacturing

[5] F. F. Noecker II, J. N. DuPont, Functionally Graded Copper – Steel Using Laser Engineered Net ShapingTM Process, Department of Materials Science and Engineering, Lehigh University, Bethlehem, PA 2002, 231–238

[6] G. N. Levy, R. Schindel, J. P. Kruth, Rapid manufacturing and rapid tooling with layer manufacturing (LM) technologies, state of the art and future perspectives, CIRP Annals - Manufacturing Technology, 52 (**2003**) 2, 589–609

[7] L. J. Swartzendruber, Binary Alloy Phase Diagrams, T. B. Massalski (ed.), 2nd ed., vol. 1, ASM, New York 1990, 1408–1409

[8] F. F. Noecker II, J. N. DuPont, Microstructural development and solidification cracking susceptibility of Cu deposits on steel: Part I, Journal of Materials Science, 42 (**2007**) 2, 495–509

[9] F. F. Noecker II, Cracking susceptibility of steel - copper alloys, Advanced Materials & Processes, 161 (**2003**) 2, 22–25

[10] D. F. Susan, J. D. Puskar, J. A. Brooks, C. V. Robino, Quantitative characterization of porosity in stainless steel LENS powders and deposits, Materials Characterization, 57 (**2006**), 36–43

[11] A. J. Pinkerton, L. Li, Direct additive laser manufacturing using gas- and water-atomised H13 tool steel powders, The International Journal of Advanced Manufacturing Technology, 25 (**2005**) 5–6, 471–479

[12] L. A. Dreval, M. A. Turchanin, A. R. Abdulov, A. A. Bondar, Thermodynamic assessment of the Cu–Fe–Cr phase diagram, Chem. Met. Alloys, 3 (**2010**), 132–139

[13] C. P. Wang, X. J. Liu, I. Ohnuma, R. Kainuma, K. Ishida, Thermodynamic database of the phase diagrams in Cu-Fe base ternary systems, Journal of Phase Equilibria and Diffusion, 25 (**2004**) 4, 320–328

[14] M. A. Turchanin, P. G. Agraval, Thermodynamics of Liquid Alloys, and Stable and Metastable Phase Equilibria in the Copper – Iron System, Powder Metallurgy and Metal Ceramics, 40 (**2001**) 7–8, 337–353

[15] C. D. Cao, Z. Sun, X. Bai, L. B. Duan, J. B. Zheng, F. Wang, Metastable phase diagrams of Cu-based alloy systems with a miscibility gap in undercooled state, Journal of Materials Science, 46 (**2011**) 19, 6203–6212

[16] C. P. Wang, X. J. Liu, I. Ohnuma, R. Kainuma, K. Ishida, Phase equilibria in Fe-Cu-X (X: Co, Cr, Si, V) ternary systems, Journal of Phase Equilibria, 23 (**2002**) 3, 236–245

[17] A. Munitz, Liquid separation effects in Fe-Cu alloys solidified under different cooling rates, Metallurgical Transactions B, 18 (**1987**) 3, 565–575

[18] Y. Z. Chen, F. Liu, G. C. Yang, X. Q. Xu, Y. H. Zhou, Rapid solidification of bulk undercooled hypoperitectic Fe–Cu alloy, Journal of Alloys and Compounds, 427 (**2007**) 1–2, L1–L5

[19] R. Monzen, T. Tada, T. Seo, K. Higashimine, Ostwald ripening of rod-shaped α-Fe particles in a Cu matrix, Materials Letters, 58 (**2004**) 14, 2007–2011

[20] M. B. Robinson, D. Li, T. J. Rathz, G. Williams, Undercooling, liquid separation and solidification of Cu-Co alloys, Journal of Materials Science, 34 (**1999**) 15, 3747–3753